AMPLIFICATION OF INTERSTELLAR MAGNETIC FIELDS BY SUPERNOVA-DRIVEN TURBULENCE

DINSHAW S. BALSARA,[1] JONGSOO KIM,[2] MORDECAI-MARK MAC LOW,[3] AND GRANT J. MATHEWS[1]

ABSTRACT

Several lines of evidence suggest that magnetic fields grow rapidly in protogalactic and galactic environments. However, mean field dynamo theory has always suggested that the magnetic fields grow rather slowly, taking of order a Hubble time to reach the observed values. The theoretical difficulties only become worse when the system has a high magnetic Reynolds number, as is the case for galactic and protogalactic environments. The discrepancy can be reconciled if fast processes for amplifying the magnetic field could operate. Following the 2001 work of Balsara and coworkers, we show that an interstellar medium that is dominated by realistic energy input from supernova explosions will naturally become a strongly turbulent medium with large positive and negative values of the kinetic helicity. Even though the medium is driven by compressible motions, the kinetic energy in this high Mach number flow is mainly concentrated in solenoidal rather than compressible motions. These results stem from the interaction of strong shocks with each other and with the interstellar turbulence they self-consistently generate in our model. Moreover, this interaction also generates large kinetic helicities of either sign. The turbulent flow that we model has two other characteristics of a fast dynamo: magnetic energy growth independent of scale and a growth time that is comparable to the eddy turnover time. This linear phase of growth permits the field to grow rapidly until the magnetic energy reaches about 1% of the kinetic energy. At that stage, other astrophysical processes for producing magnetic fields can take over. Energetics, power spectra, statistics, and structures of the turbulent flow are studied here. Shock-turbulence interaction is shown to be a very general mechanism for helicity generation and magnetic field amplification, with applicability to damped Lyα systems, protogalaxies, the Galaxy, starburst galaxies, the intracluster medium, and molecular clouds.

Subject headings: ISM: magnetic fields — supernovae: general — turbulence

1. INTRODUCTION

Ever since the early observation of finite rotation measures in high-redshift quasars by Kronberg & Perry (1982), Perry et al. (1993), and Kronberg (1995), there has been considerable interest in the formation of magnetic fields in such environments. This interest has increased as a result of the observation of fields of a few μG in damped Lyα systems at $z = 2$ by Wolfe et al. (1992). The result is doubly interesting. First, it shows that high-redshift systems that may or may not have a well-established differential rotation still manage to form magnetic fields with field strengths comparable to our present Galactic field strength (see Rand & Kulkarni 1989; Beck et al. 1996). Second, it shows that the field reaches this strength extremely swiftly compared to the several Gyr *e*-folding times estimated for mean field dynamos (e.g., Ferrière & Schmitt 2000).

A study of the magnetic field in our own Galaxy yields further insights. Rand & Kulkarni (1989) studied the magnetic field within a few kpc of the solar neighborhood. They found that the mean magnetic field had a magnitude of 1.6 μG, while the fluctuating component of the magnetic field was estimated to have a strength of about 5 μG. Beck et al. (1996) carried out similar observations of the Galaxy and nearby galaxies. They too found that the fluctuating component of the magnetic field had a strength that was comparable to the mean field. These observations, however, only probe the fluctuating field on a very limited range of length scales. Nevertheless, the presence

of a fluctuating component may be explained as resulting from turbulent motions in the interstellar medium (ISM). Observations by Spangler (1999), Haverkorn et al. (2000), and Gaensler et al. (2001) probe the structure of the ISM on a much larger range of length scales. The latter observations further support the idea that the ISM might indeed be turbulent, although they do not directly probe the structure of the magnetic field. Minter & Spangler (1996) observed rotation and emission measures for a small section of the sky to deduce the spectrum of magnetic field fluctuations on scales smaller than 100 pc, finding evidence for a turbulent component in the magnetic field. Fosalba et al. (2002) used starlight polarization to come to a similar conclusion. Han et al. (2004) used pulsar dispersion and rotation measurements to deduce the energy spectrum of the interstellar magnetic fields on scales spanning 0.5–15 kpc. The data suggest that the turbulence is three-dimensional on smaller scales but becomes two-dimensional on larger scales. There is no current observational evidence for the structure of magnetic fields at protogalactic length scales. However, there is adequately strong evidence for vigorous star formation activity leading to turbulence in such environments, which suggests that magnetic field fluctuations would develop on a range of length scales in those systems too. It is therefore interesting to study the formation and evolution of magnetic fields in such turbulent environments.

The papers by Field et al. (1969), Cox & Smith (1974), and McKee & Ostriker (1977), when taken together, have shown that the three-phase structure of the ISM is primarily sustained by energetic input from supernova (SN) explosions and winds from OB stars. This is because an accounting of the energetic input into the ISM shows that SNe and winds, in that order, are the dominant sources of mechanical input into the turbulent ISM (see reviews by Mac Low & Klessen 2004; Elmegreen & Scalo

[1] Center for Astrophysics, Department of Physics, University of Notre Dame, Notre Dame, IN 46556; dbalsara@nd.edu, gmathews@nd.edu.
[2] Korea Astronomical Observatory, 36-1 Whaam-dong, Yuseong-Gu, Taejon 305-348, Korea; jskim@kao.re.kr.
[3] Department of Astrophysics, American Museum of Natural History, Central Park West at 79th Street, New York City, NY 10024.

2004; Scalo & Elmegreen 2004). Balsara et al. (2001a, hereafter BBC01) have studied the interaction of three-dimensional SN remnants with a turbulent, magnetized ISM. Korpi et al. (1999) carried out low-resolution simulations of SN-driven, magnetized, interstellar turbulence. Kim et al. (2001) studied the energetics, structure, and spectra of such a turbulent medium with substantially higher resolution simulations. Balsara & Kim (2004) made a detailed study of the role of good numerical methods in enabling a faithful representation of magnetic field amplification in such SN-driven turbulence. Mac Low et al. (2004) have studied the thermodynamic nature of interstellar turbulence with SNe being the dominant energy input mechanism. The simulation work cited above clearly indicates that the turbulence is supersonic and that compressibility effects produce a range of densities. It is the purpose of this paper to make a detailed study of the magnetic field amplification in such a turbulent, compressible, magnetized ISM with energy input being provided by SN explosions. Understanding this problem may yield insights into magnetic field generation in primordial galaxies, starburst galaxies, our Galaxy, and perhaps even our Galactic center.

Ruzmaikin et al. (1988) have used mean field dynamo theory to study the problem of magnetic field generation in the Galaxy. Mean field dynamo theory is based on the early work of Parker (1971) and Steenbeck et al. (1966), who formulated the problem for incompressible magnetohydrodynamics (MHD) by assuming that one could effect a split in length scales. On small scales, the magnetic fields and helical fluid motions are presumed to be driven by several forms of gentle convective motion. These gentle helical motions, along with the mean shear in the Galactic rotation curve, produce growth of the mean field on large scales. To sustain a persistent dynamo, it is therefore important to find robust mechanisms for helicity generation in the Galaxy. Ferrière (1993a, 1993b, 1995, 1998) showed that SN explosions and superbubbles in the sheared and stratified Galactic ISM could provide one possible mechanism for helicity generation. This mechanism for generating helicity was used in conjunction with the theory for the α-ω dynamo by Ferrière & Schmitt (2000) to predict growth times for the mean Galactic field. The time of growth for the large-scale magnetic field was found to be about 1.8 Gyr for most of their models, suggesting that the Galactic magnetic field has currently reached a value that is close to saturation. The large times of growth indicate that the Galactic magnetic field has undergone no more than a few e-foldings over a Hubble time. Therefore, for the field to have reached its current strength in the Galaxy, mean field dynamo theory indicates that the proto-Galaxy should have started with a magnetic field that was $\sim 1.5 \times 10^{-9}$ G. However, simulations of the Biermann (1950) battery effect and its ability to produce strong seed fields in clusters and protogalactic environments show that the proto-Galactic seed field should be much smaller (see Kulsrud et al. 1997).

The simulations of Kulsrud et al. (1997) find that the proto-Galactic fields were $\sim 10^{-21}$ G. This suggests that it might be useful to look for field amplification mechanisms that go beyond the limiting assumptions of mean field dynamo theory. For example, mean field dynamo theory is predicated on slow, almost incompressible motions that take place in a nonclumpy, almost smooth plasma. Observations suggest that the ISM has supersonic motions that produce strong local compressions. Furthermore, the highly compressible equation of state of the ISM gives it a strong tendency to form clumpy clouds of cold gas, each of which has its own internal turbulence. A thorough study of blast wave interactions and their role in generating kinetic helicity and amplifying magnetic fields in strongly compressible, clumpy, radiatively cooled and heated, turbulent media has never been undertaken. We begin such a study here.

Kulsrud & Anderson (1992, hereafter KA92) pointed out that there is a further problem with mean field dynamo theory when it is applied to galactic/protogalactic environments. KA92's calculations are based on Kraichnan & Nagarajan's (1967) Lagrangian history direct interaction approximation for incompressible MHD turbulence. KA92 point out that the magnetic Reynolds number (Re_m) of our Galaxy is very large, $\mathrm{Re}_m \sim 10^{16}$. KA92 conclude that the large value of Re_m implies that mean field dynamo theory is not applicable to our Galaxy. The high value for Re_m causes turbulent velocity fluctuations and turbulent magnetic field fluctuations to develop on small scales. These small-scale fluctuations in the magnetic field grow rapidly, and the calculations of KA92 suggest that the small-scale magnetic energy should grow rapidly to the point at which it is in equipartition with the kinetic energy. This, in turn, was claimed to quench the turbulence, thereby arresting the growth of large-scale magnetic fields. One of the suggestions that comes out of the work of KA92 is that it is very important to study the growth of magnetic fields in systems in which there is a considerable separation between the large scales and the small scales. Thus, simulating the growth of magnetic fields in computational domains that are large enough to permit a separation between the large scales and the small scales is a problem of great interest. KA92 also ignore the fact that interstellar turbulence is driven by strong SN shocks. These shocks are strong enough to overpower the small-scale saturation. While KA92 and Howard & Kulsrud (1997) have shown the importance of a clumpy medium, they have not paid much attention to the role of strong shocks when they interact with such a clumpy ISM. We show the importance of such interactions in the next paragraph.

As seen from the work of Ferrière (1993a, 1993b, 1995, 1998), the existence of robust mechanisms for generating kinetic helicity is of great interest in magnetic field amplification. McKenzie & Westphal (1968) were the first to realize the importance of shocks and their ability to amplify turbulence when they interact with it. McKee & Zweibel (1995) came to a similar realization in the astrophysical literature. Samtaney & Zabusky (1994) used shock polar analysis to calculate scaling relations for vorticity generation when shocks interact with density inhomogeneities in two dimensions. They found that increasing shock Mach numbers or increasing density contrasts enhances vorticity generation at the shocks. While kinetic helicity cannot be generated by two-dimensional flows, a robust mechanism for vorticity generation in two dimensions will produce helicity when turbulent motions in the third dimension are allowed. While the amplification of turbulence that is demonstrated in McKenzie & Westphal (1968) is based on a linear analysis, the demonstration of vorticity generation by Samtaney & Zabusky (1994) is an inherently nonlinear calculation. As a result, the generation of helicity when shocks interact with turbulence should be a robust conclusion, even in the nonlinear regime. BBC01 showed that the interaction of SN shocks with interstellar turbulence amplifies postshock turbulence and is also a source of helicity generation. They showed that strong fluctuations in kinetic helicity of either sign are produced when the turbulence is homogeneous and isotropic. SN remnants and superbubbles can interact with large-scale density contrasts in the ISM, resulting in a breakout of the remnant's cavity (e.g., Magnier et al. 1996; Williams et al. 1999). This is different from the conventional description for

the terminal evolution of a remnant by Cox & Smith (1974), which postulates that the remnant begins to merge gradually with the ambient medium when its expansion speed equals the ambient medium's sound speed. However, various instability mechanisms, such as the Vishniac overstability (Vishniac 1983), the Rayleigh-Taylor instability during breakout (e.g., Mac Low & McCray 1988), and gravitational instability (e.g., McCray & Kafatos 1987), might be other mechanisms for helicity production in supersonic, compressible, clumpy ISM. One must therefore pay attention to those other sources of helicity production.

There is also a substantial amount of recent interest in studying magnetic field generation in helically driven turbulence. Such turbulence would constitute an α^2 dynamo. Such a study of the turbulent dynamo with scale separation was reported by Zeinecke et al. (1998, hereafter ZPP98) for the case of incompressible MHD and was extended to compressible MHD using even larger computational domains by Balsara (2000). Both ZPP98 and Balsara (2000) studied a turbulent MHD system that was driven with motions that had the maximal amount of kinetic helicity with a single sign. They found that the initial magnetic field energy grew exponentially with a constant growth rate. They called this epoch the regime of linear growth. As the field strength grew, they found that the rate of growth of the magnetic energy was diminished when the magnetic energy reached a strength of $\sim$2% of the kinetic energy. However, the growth of the field persisted at a slower rate, so that the magnetic field underwent what they called a quasi-linear phase of growth. This happened despite the fact that the small-scale magnetic field strength was less than an order of magnitude away from equipartition with the velocity field. Both ZPP98 and Balsara (2000) were able to show that systems existed that could approach equipartition between the magnetic energy and the kinetic energy and yet show large-scale field growth as long as the helical driving was persistent. While the ZPP98 and Balsara (2000) simulations were maximally helical, Maron & Blackman (2002) have done incompressible simulations with fractionally helical driving and found that when the fraction of helical driving exceeds a certain value, large-scale field growth takes place. Galloway & Proctor (1992) studied the evolution of a kinematic dynamo in a flow with Lagrangian chaos and zero mean helicity and found evidence for magnetic field amplification. Since Maron & Blackman (2002) did not analyze the Lagrangian chaos in their streamlines, it is difficult to connect the two results. All the simulations cited in this paragraph are based on idealized forms of driving that were put in by hand. None of them were based on SN-driven turbulence of the sort that occurs naturally in the ISM. Thus, it is of interest to examine what SN-driven turbulence might do.

The driven turbulence studied by ZPP98 and Balsara (2000) was motivated by a class of theories known as fast dynamo theories. Fast dynamo theories specifically apply to the high-Re_m regime and were first proposed by Vainshtein & Zeldovich (1972). Childress & Gilbert (1995) have reviewed such theories. They find that the magnetic field can grow very rapidly in certain high-Re_m systems that have a net helicity. The amplification of the magnetic field takes place via a "stretch, twist, and fold" mechanism. Childress & Gilbert (1995) also realized the limitations of such a forcing. Two persistent questions come through in Childress & Gilbert (1995). (1) Are there physical systems that can produce large helicity fluctuations of either sign so that the overall helicity of the system is zero? (2) Can one have fast magnetic field growth in such systems? The simulations that are presented in the current paper show both that the ISM is a physical system and that it might naturally

produce strong helicity fluctuations of either sign. In a subsequent paper, we will address the issue of rapid flux growth and its relation to dynamical chaos.

In § 2 we describe the physical system and provide numerical details. In § 3 we study the energetics associated with magnetic field growth in such systems. In § 4 we study the spectra of the magnetic and kinetic energy. In § 5 we study turbulent structures and statistics that result in the system being studied. In § 6 we offer a discussion and some conclusions.

2. DESCRIPTION OF THE NUMERICAL MODEL

In the first part of this section we describe the basic equations and the numerics used. In the second part we describe the simulations.

2.1. Basic Equations

We solve the three-dimensional MHD equations using conserved quantities with heating and cooling adjusted for the ISM:

$$
\frac{\partial}{\partial t}
\begin{pmatrix}
\rho \\
\rho v_x \\
\rho v_y \\
\rho v_z \\
\epsilon \\
B_x \\
B_y \\
B_z
\end{pmatrix}
+ \frac{\partial}{\partial x}
\begin{pmatrix}
\rho v_x \\
\rho v_x^2 + P + B^2/8\pi - B_x^2/4\pi \\
\rho v_x v_y - B_x B_y/4\pi \\
\rho v_x v_z - B_x B_z/4\pi \\
(\epsilon + P + B^2/8\pi)v_x - B_x(\boldsymbol{v}\cdot\boldsymbol{B})/4\pi \\
0 \\
(v_x B_y - v_y B_x) \\
-(v_z B_x - v_x B_z)
\end{pmatrix}
$$

$$
+ \frac{\partial}{\partial y}
\begin{pmatrix}
\rho v_y \\
\rho v_x v_y - B_x B_y/4\pi \\
\rho v_y^2 + P + B^2/8\pi - B_y^2/4\pi \\
\rho v_y v_z - B_y B_z/4\pi \\
(\epsilon + P + B^2/8\pi)v_y - B_y(\boldsymbol{v}\cdot\boldsymbol{B})/4\pi \\
-(v_x B_y - v_y B_x) \\
0 \\
(v_y B_z - v_z B_y)
\end{pmatrix}
$$

$$
+ \frac{\partial}{\partial z}
\begin{pmatrix}
\rho v_z \\
\rho v_x v_z - B_x B_z/4\pi \\
\rho v_y v_z - B_y B_z/4\pi \\
\rho v_z^2 + P + B^2/8\pi - B_z^2/4\pi \\
(\epsilon + P + B^2/8\pi)v_z - B_z(\boldsymbol{v}\cdot\boldsymbol{B})/4\pi \\
(v_z B_x - v_x B_z) \\
-(v_y B_z - v_z B_y) \\
0
\end{pmatrix}
$$

$$
=
\begin{pmatrix}
0 \\
0 \\
0 \\
0 \\
-\rho^2 \Lambda(T) + \rho \Gamma_0 \\
0 \\
0 \\
0
\end{pmatrix},
$$

where $\epsilon = \rho v^2 /2 + P/(\gamma - 1) + B^2 /8\pi$ is the total energy of the plasma. In all our simulations, the ratio of specific heats γ was set to 5/3.

The heating is representative of photoelectric and cosmic-ray heating. The cooling is obtained from the work of Raymond & Smith (1977). As a result, the cooling function used in this work does not incorporate some of the molecular cooling terms, and especially not the heating effects of polycyclic aromatic hydrocarbons, as shown in Wolfire et al. (1995, 2003). As a result, the current round of simulations have the requisite physics to produce the hot and the warm phases of the ISM but not the cold phase. Inclusion of the cold phase, along with all the extra physics and numerics that are needed for its inclusion, will be the topic of subsequent papers. Because we have chosen solar metallicities in this work, the simulations are directly applicable to the Galactic ISM. However, it is useful to point out that Mushotzky & Loewenstein (1997) have observed several clusters and found them to have a metallicity that is $\sim$0.3 of our solar value. Likewise, Churchill & Le Brun (1998) and Ledoux et al. (2002) find metallicities in damped Lyα systems that are close to solar values. Thus, this work will also have applicability to these other systems.

The equations are solved on a three-dimensional Cartesian mesh using the total variation diminishing (TVD) methods described in Balsara & Spicer (1999a, 1999b), Balsara (2004), and Balsara & Kim (2004). Specifically, we use the fast TVD algorithm drawn from the RIEMANN code that was described in Balsara (2004) and calibrated for the present application in Balsara & Kim (2004). The solution methods are all based on higher order Godunov schemes that are known to produce effective magnetic Prandtl numbers of unity. While that may be different from the Galactic value, these methods are the only known methods that will robustly integrate the physics of strong shocks that needs to be represented for this scientific problem.

2.2. *Description of Simulations*

The simulations evolve small cubical patches of the ISM that are 200 pc on an edge. This size is chosen because a distance of 100 pc is smaller than the scale height of the ISM. Hence, the simulations represent a patch of the ISM in the midplane of the Galaxy. Balancing heating with cooling at a specified density and temperature enables us to set Γ_0, the assumed rate of photoelectric and cosmic-ray heating. Thus, the mean density and temperature are two of the parameters that specify these simulations. We start with a very small, uniform, seed magnetic field, which also constitutes one of the parameters that specifies the simulations. The SN rate is another determining parameter in these simulations. In this work we adopt a fiducial SN rate in our Galaxy of two SN explosions per century. Thus, a Galactic SN rate corresponds to one SN exploding every 1.26 Myr in our computational domain. For our purposes there is no need to distinguish between Type I and Type II SNe. Thus, the SN rate is specified as a multiple of this Galactic SN rate. As a first approximation, the SNe explode in random locations in the computational domain. For our present computational purposes, an SN explosion imparts 10^{51} ergs of thermal energy within a radius of 5 pc of the randomly selected explosion site. That energy pulse then evolves in time. The SN rate determines the interval of time between successive SNe. Extensive code tests were done to ensure that isolated SN remnants that were initialized with a radius of 5 pc evolved spherically in a uniform, unmagnetized medium. To retain physical consistency across simulations, the
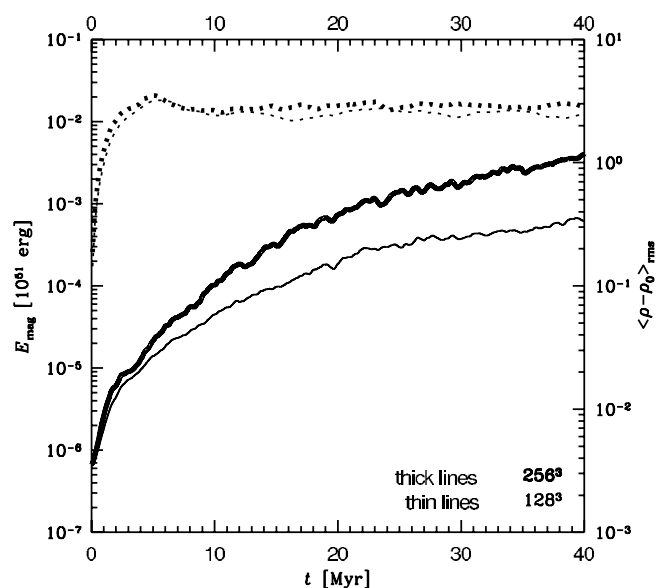

Fig. 1.—Log of magnetic energy (*solid lines*) and rms density (*dotted lines*) vs. time for runs at 128^3 and 256^3 zone resolution. Thick and thin lines indicate the high- and low-resolution simulations, respectively.

same initial radius of 5 pc was used for the remnants on all the meshes that were used in this work.

The simulations tend to be very long running, even on the fastest parallel supercomputers, with typical run times that exceed 10^5 CPU hr. This is so because for a field growth experiment, one needs to run the simulations for several eddy turnover times, resulting in almost 1000 SNe going off in the course of a run. The short time steps needed to follow each individual SN remnant along with the large number of explosions makes these simulations very challenging. We also wish to have results that are close enough to the converged results of an infinitely fine mesh. Therefore, we present results from two identical simulations that have resolutions of 128^3 and 256^3 zones. If the two simulations show roughly similar systematic behavior, we can conclude that the answers we obtain from the higher resolution simulation are close enough to the converged answers. Initially, we carried out three simulations at 128^3 zone resolution with 8, 12, and 40 times the Galactic SN rate. The most interesting of these simulations was then repeated on a 256^3 zone mesh. That simulation had a density of 1 amu cm^{-3}, a mean temperature of 10,000 K, an initial magnetic field energy that was 2×10^{-6} times smaller than the thermal energy, and an SN rate that was 8 times larger than our adopted Galactic rate. The higher SN rate was necessary for producing appreciable field growth in a sufficiently short simulational time. Lower SN rates will also produce field growth, albeit at a somewhat slower rate. Moreover, such high SN rates are also consistent with those expected to occur in starburst and protogalactic environments.

3. STUDY OF THE ENERGETIC ASPECTS OF THE TURBULENCE

3.1. *Energy Growth Rates*

Figure 1 shows the growth of magnetic energy and rms density fluctuations for runs with 128^3 and 256^3 zones for the first 40 Myr of simulation time. Both runs show a very rapid initial increase in the magnetic energy during the first 5 Myr. This initial growth does not represent the growth of magnetic
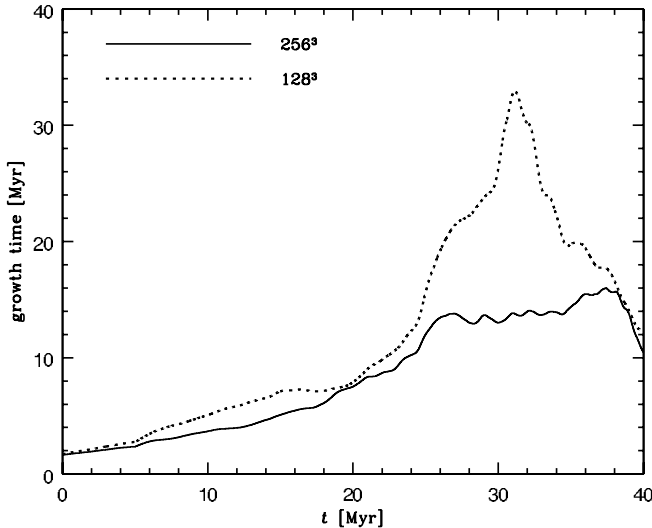
Fig. 2.—Growth time smoothed with a 10 Myr window function for the runs in Fig. 1.

energy in steady state turbulence. Instead, the first 5 Myr in both simulations correspond to the time it takes for the SN-driven forcing to produce well-developed turbulence, as shown by the saturation of the rms density fluctuations. The first 5 Myr, therefore, correspond to the time it takes for every parcel of gas in the simulation to be fully processed in at least one SN. A higher rate of SNe results in a faster onset of fully developed turbulence, and a lower rate of SNe results in a slower onset of fully developed turbulence. To verify that we have fully developed turbulence in the computational domain, we compared the velocity spectrum at 5 Myr with the velocity spectrum at later times and found that the spectral shape remained unchanged. The growth of magnetic energy after 5 Myr, despite the saturation of the rms density fluctuations, allows us to safely assert that the magnetic field growth does occur in steady state turbulence and is not due to rms density fluctuations that increase with time.

After the first 5 Myr the field energy continues to grow almost monotonically, increasing by over 2 orders of magnitude in the course of the simulation. The temporal evolution of magnetic energy, shown in Figure 1, displays jitters over very short time intervals. To eliminate the influence of these jitters in quantifying the growth time of the magnetic energy, we used a sliding window of 10 Myr to measure the best-fit value of the growth time. The growth time is the time required by the field to increase by 1 e-folding. In Figure 2 we plot growth time as a function of simulation time for both runs. We see from Figure 2 that the magnetic field in the 256^3 zone run has growth time fluctuating from 4 to 16 Myr in the time interval from 10 to 40 Myr. We also see that the growth time is not a constant but rather fluctuates in a broad range as a function of time. The fluctuations appear to be a consequence of the random locations of the SNe.

It is very instructive to compare the 128^3 and 256^3 zone simulations. From Figure 1 we see that the 128^3 zone simulation has a slightly lower value of the magnetic energy than the 256^3 zone simulation. This owes to the fact that the 256^3 zone simulation has many more zones than the 128^3 zone simulation. Hence, there is a lot more small-scale magnetic structure that can be represented in the 256^3 zone simulation that is not present in the 128^3 zone simulation. The 256^3 zone simulation therefore seems to contain more magnetic energy

than the 128^3 zone simulation. This is simply a manifestation of the fact that neither of the two simulations has enough resolution to permit a long inertial range to form. Nevertheless, the curves of growth do track each other, indicating that there is a rough agreement between the two simulations. Likewise, both simulations show growth of magnetic energy over several orders of magnitude, indicating that the growth of magnetic energy in our simulated ISM is a robust conclusion. From Figure 2 we also see that the growth times for the two simulations track each other for a good fraction of the interval. The only exception is the interval between 25 and 36 Myr. On detailed examination of the placement of successive SN explosions, we found that the random number generator produced SN explosions that were contiguous to each other at 25 Myr. On the larger mesh we found that the explosions still have sufficient distance between each other that one explosion did not go off within the cavity of the previous explosion. On the smaller mesh, that was not the case, causing unusually high rates of heating and a subsequent slowdown in the growth of the magnetic field. This shows us two things: First, it shows that there are numerically induced differences that can be triggered in this problem that require careful subsequent interpretation. Second, it shows us that SN explosions going off within the cavities of previous remnants are almost inevitable, especially when the SN rate is high enough. When such episodes occur, one might experience a local decrease in the growth rate of the magnetic field. This point is expanded on below in § 3.4.

Figure 1 shows that the energy in the magnetic field increases by over 2 orders of magnitude in the course of the simulation but does not reach equipartition. In fact, by the end of the simulation the field energy is still only 1% of its equipartition value. We do, however, see that the field is still growing at a robust rate toward the end of the simulation. Using more idealized simulations, ZPP98 and Balsara (2000) both found that once the magnetic energy reaches 2% of the kinetic energy, the growth rate of the magnetic energy slows down markedly. They called this the quasi-linear phase of evolution. The field underwent a protracted phase of quasi-linear evolution (with a much reduced growth rate) before the magnetic energy reached rough equipartition with the kinetic energy. For that idealized problem it was very important to clearly demonstrate that turbulent flows could indeed amplify the field energy to equipartition. In our present simulations we too seem to have reached a stage in which the magnetic energy has reached about 1% of the kinetic energy by the end of 40 Myr. In this problem it is not important to demonstrate that equipartition is achieved. This is because once the field strength has been raised to appreciable levels in a protogalaxy, slower processes, such as the α-ω dynamo, can take over and increase the large-scale field even further. We also factor in the practical consideration that our higher resolution simulation took over 4 months to run on a medium-sized PC cluster. As a result, we will leave the issue of approach to equipartition and the role of other astrophysical processes in producing further field growth for future work.

3.2. Similarities to a Fast Dynamo

In a subsequent paper we will analyze the Lyapunov exponents associated with streamlines, thereby demonstrating the Lagrangian chaos in the SN-driven turbulence. We will also make a detailed connection between the rapid growth of magnetic flux and various indicators of Lagrangian chaos in the flow. ZPP98 and Balsara (2000) argue that certain well-designed
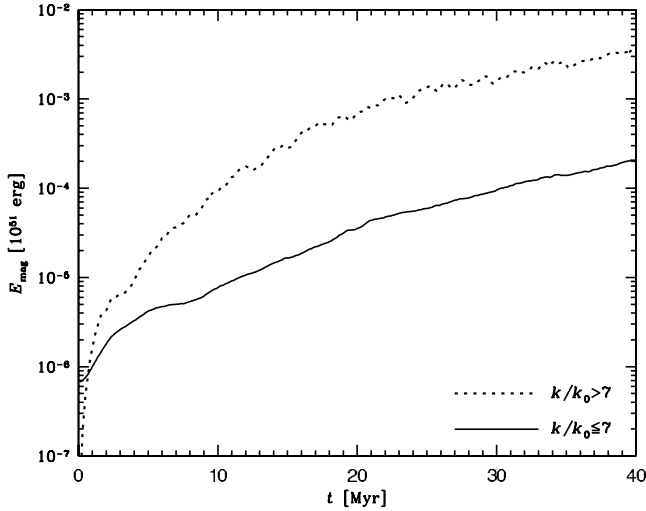
Fig. 3.—Growth of magnetic energy in the 256^3 zone simulation on all scales smaller (*dotted line*) and larger (*solid line*) than the typical size of an SN remnant, 30 pc, equivalent to $k/k_0 = 7$.

Fig. 4.—Time evolution of spectral modes with wavenumber $k/k_0 = 3$ (*solid line*), 5 (*dotted line*), 9 (*short-dashed line*), and 11 (*long-dashed line*). The first two modes represent length scales larger than the size of an SN remnant (roughly $k/k_0 = 7$), while the second two are smaller.

energy considerations provide evidence of a fast dynamo. Since this section is devoted to energy considerations, we repeat the same for our own simulations below.

First is a growth time for magnetic energy comparable to the eddy turnover time. The density-averaged rms velocity in our simulations $v_{rms} \sim 12$ km s^{-1}. Using a median SN remnant radius $R \sim 30$ pc, we find an effective eddy turnover time $R/v_{rms} \sim 2.5$ Myr, of the same order as the growth times shown in Figure 2. ZPP98 mention that the existence of a magnetic energy growth rate that is comparable to the eddy turnover time is one of the circumstantial pieces of evidence that a fast dynamo is operating. The growth times we find in this paper are much shorter than the $\sim$1.8 Gyr growth times that were estimated by Ferrière & Schmitt (2000) for the α-ω dynamo driven by Galactic superbubbles.

A second feature is a magnetic energy growth rate that is independent of scale, which does not arise in the classical α^2 dynamo. ZPP98 and Balsara (2000) also used spectral analysis to show that the magnetic energy on long scales and short scales grew at the same rate in the linear regime. They showed that a scale-independent growth rate provides another piece of evidence that a fast dynamo-like behavior was being observed. Owing to the simplicity of their forcing term, ZPP98 and Balsara (2000) could clearly identify a length scale on which they forced the turbulent flow. They identified the long scales as scales that exceeded their forcing scale, and short scales as the rest. In the present problem, the size of an SN remnant takes the place of the forcing length scale. Because SN remnants occupy a range of length scales, one cannot identify a single forcing scale in the present problem. We therefore identify the radius of a typical remnant, 30 pc, as the scale at which we distinguish between large and small scales. A length of 30 pc corresponds to one-seventh of our computational domain. Figure 3 shows the growth of magnetic energy on all scales that are larger than 30 pc (*solid line*) and on all scales that are smaller than 30 pc (*dashed line*). From 5 to 20 Myr we do see that the short scales grow somewhat faster than the longer scales, owing to the fact that the direct cascade of magnetic energy has shorter eddy turnover times and can establish itself much more rapidly. However, past 20 Myr we see that the two curves do indeed grow at the same rate for an appreciable length of time.
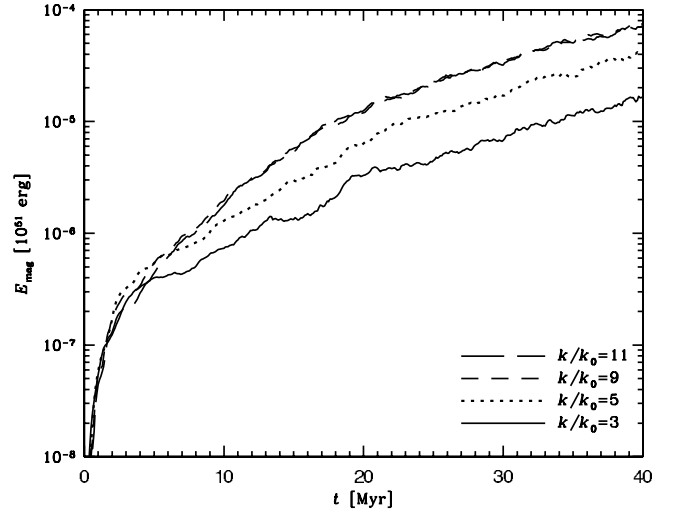
While the ad hoc split into small and large length scales in this problem may seem arbitrary, it is possible to analyze the rate of growth for several of the individual spectral modes in the problem. This is done in Figure 4, which shows the temporal evolution of the $k = 3$ and 5 spectral modes. These represent length scales that are decidedly larger than the size of an SN remnant. We also plot the temporal evolution of the $k = 9$ and 11 spectral modes, which represent length scales that are decidedly smaller than the size of an SN remnant. It is easily seen that past 20 Myr the large-scale modes and the small-scale modes grow at the same rate.

3.3. *Kinetic and Magnetic Helicity*

While the mean kinetic helicity in this problem remains zero, it is interesting to ask how it evolves. We also realize that the magnetic energy grows with time in this problem. The strong connection between the inverse cascade of magnetic helicity and the problem of magnetic field amplification was first pointed out by Pouquet et al. (1976). Balsara & Pouquet (1999) have also carried out simulations of the inverse cascade of magnetic helicity for the compressible case. As a result, the evolution of magnetic helicity is also a topic of interest. Figure 5 plots the evolution of the rms fluctuations in the kinetic and magnetic helicities on the same plot as a function of time. The kinetic helicity is given by $\boldsymbol{v} \cdot \nabla \times \boldsymbol{v}$. The magnetic helicity is given by $\boldsymbol{A} \cdot \boldsymbol{B}$, where $\boldsymbol{B} = \nabla \times \boldsymbol{A}$. The kinetic helicity shows a very spiky behavior, where each spike corresponds to an SN explosion, supporting the suggestion that the interaction of the remnants with the turbulent ISM is a strong source of kinetic helicity. We also see that the rms fluctuation in the kinetic helicity does not grow, unlike the rms fluctuation in magnetic helicity, which does. This is consistent with the fact that the magnetic energy grows with time, while the kinetic energy does not.

3.4. *Effect of the SN Explosion Rate*

The simulations that we have discussed so far all had an SN rate of 8 times Galactic. Will this mechanism persist at much higher SN rates? Many real-world astrophysical effects could
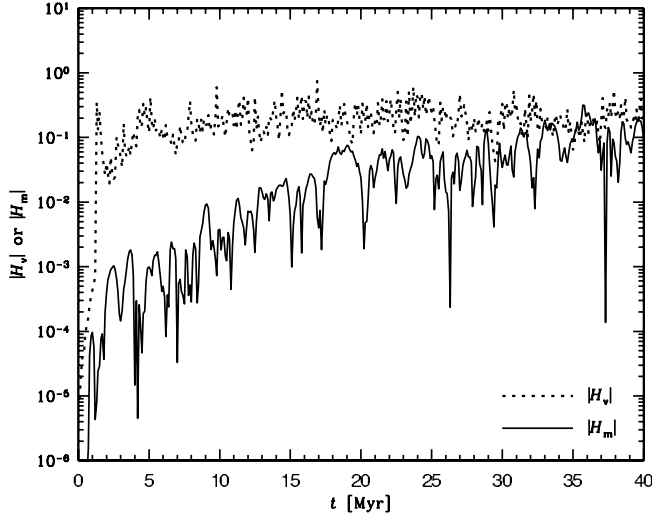
Fig. 5.—Evolution of rms fluctuations in the kinetic (*dotted line*) and magnetic (*solid line*) helicities as a function of time.

change the answer that we attempt to give here. For example, stratification of the disks in real galaxies will result in the hot phase of the ISM blowing out via bubbles and chimneys, as observed in NGC 891 (Rand et al. 1990). However, over the course of our simulations, we did explore the conditions that are needed for the present mechanism to operate via a brief parameter study. Figures 6a–6c show the evolution of thermal, kinetic, and total energy as a function of time in runs with SN rates of 8, 12, and 40 times the Galactic value, while Figure 6d shows the evolution of magnetic energy in the last run. When the SN rate exceeds a critical rate, we expect SN explosions to occur frequently within the cavities of previous remnants. When that happens, we expect the magnetic energy growth to be quenched. We can only bracket the critical rate with the simulations in hand. In Figures 6a and 6b we see that the runs reach thermal equilibrium, at which the energy input from SNe balances the energy loss from radiative cooling. In those cases we find robust growth of the magnetic field. Note, however, that the magnetic energy is substantially smaller than the kinetic and thermal energies all through the evolution of these simulations. Thus, one should not expect to see a secular growth in total energy as a result of growth in magnetic energy. In Figure 6c a thermal runaway sets in as all the gas is heated to temperatures at which radiative cooling becomes inefficient. The thermal runaway is initiated at 2 Myr, but it
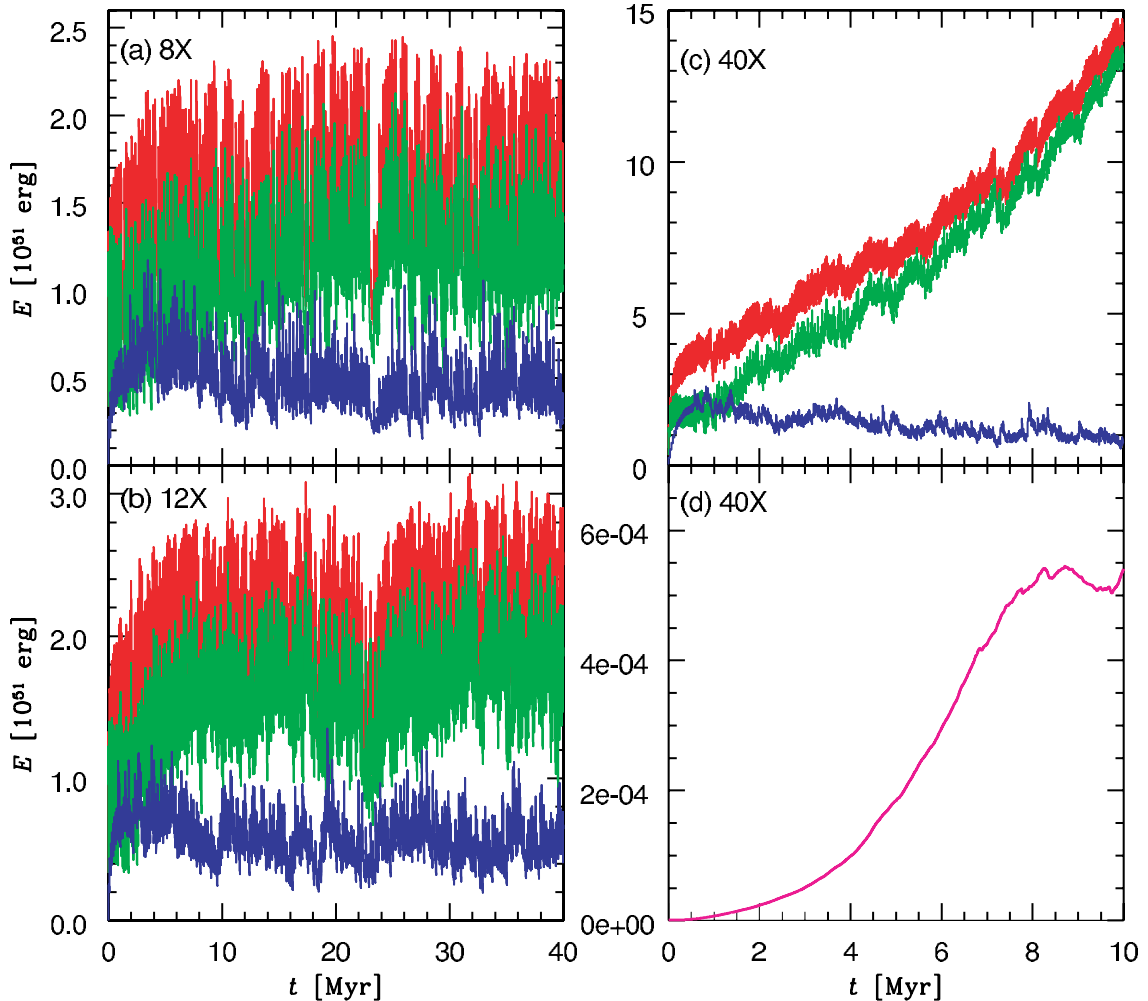

Fig. 6.—Time evolution of thermal (*green*), kinetic (*blue*), and total (*red*) energy in runs with SN rates of (*a*) 8, (*b*) 12, and (*c*) 40 times the present Galactic value, as well as (*d*) the magnetic energy in the last of these runs.
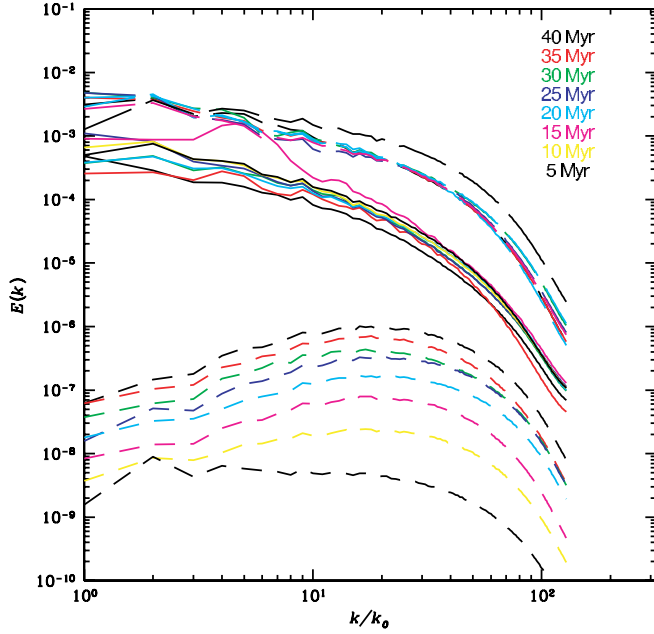
FIG. 7.—Spectra for the density-averaged kinetic (*solid lines*) and magnetic (*short-dashed lines*) energies and fluid density (*long-dashed lines*) at several different times in the 256^3 zone run. Different epochs are shown with different colors. We see that the kinetic energy and fluid density saturate, while the magnetic energy keeps growing.

FIG. 8.—Spectrum for the compressible (*solid lines*) and solenoidal (*dotted lines*) parts of the velocity field at various times from the 256^3 zone run. Different epochs are shown with different colors. We find the surprising result that except for some of the largest length scales, the solenoidal part of the velocity spectrum overwhelms the compressible part of the velocity spectrum by more than an order of magnitude.

takes till about 8 Myr before most of the gas is converted to million-degree gas, making the runaway pervasive. Figure 6*d* shows that the magnetic energy in this case does grow initially but is quenched once the thermal runaway becomes pervasive. The critical SN rate thus lies somewhere between 12 and 40 times the Galactic value for our chosen initial density and temperature.

That such a quenching should exist past some critical SN rate is easy to understand on physical grounds. The growth of field is based on helicity production when strong SN shocks interact with a predominantly warm ISM, as shown by BBC01. However, after thermal runaway, most of the ISM ceases to be warm. In fact, most of it is filled with million-degree hot gas. When an SN explosion occurs in such a hot medium, the shock quickly becomes weak and so stops producing helicity via its interaction with ambient turbulence; therefore, magnetic field amplification ceases.

4. POWER SPECTRA OF THE TURBULENCE

Having studied the bulk energetics of the system, we now turn our attention to the spectral domain. Figure 7 shows the power spectra for kinetic and magnetic energies and the density at several different times in the 256^3 zone run. The kinetic energy and the density saturate, while the magnetic energy keeps growing. The saturation of the density spectra on all scales provides further evidence that the magnetic field growth past 5 Myr is not a consequence of time-dependent rms fluctuations in the density. We see, however, that the magnetic energies have not reached equipartition even on small scales by the end of the simulation. This shows that the present simulations do not explore the saturation of turbulent field amplification. The temporal evolution of the magnetic energy closely mirrors the energetic evolution of the small- and large-scale magnetic fields that was shown in Figures 3 and 4.
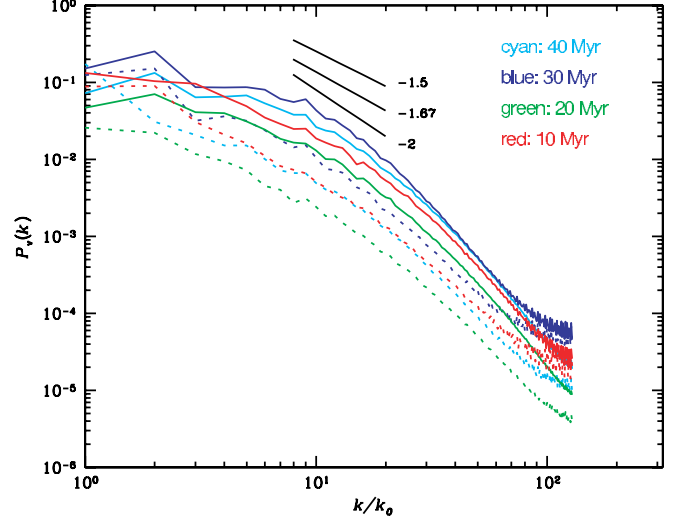
A fair bit of work has been done to study turbulence associated with strong shocks. In our calculation we drive the turbulence with very strong shocks indeed. It is therefore of some interest to analyze the kinetic energy spectrum shown in Figure 7. In Figure 8 we decompose the spectrum into its compressible and solenoidal parts. Different epochs are shown with different colors. The solid lines correspond to the solenoidal part of the velocity spectrum, and the dotted lines correspond to the compressible part of the velocity spectrum. We find the surprising result that at most length scales, the solenoidal part of the velocity spectrum overwhelms the compressible part of the velocity spectrum by almost an order of magnitude. This is quite an interesting result, given that the computations were forced with very strong shocks. Similar results for strongly forced turbulence have been reported in Passot & Pouquet (1987), Balsara & Pouquet (1999), Porter et al. (1999), Boldyrev (2002), and Vestuto et al. (2003). It is also significant that Figure 6*a* shows that the turbulence has a Mach number that is in excess of unity. Despite this high Mach number, Figure 8 shows that the turbulence can sustain strong vortical motions. Figure 8 also provides a spectral confirmation of the demonstration by BBC01 that strong shocks interacting with a clumpy and turbulent ISM can be a strong source of kinetic helicity fluctuations. We put three line segments with slopes of -1.5, -1.67, and -2 in Figure 8 that correspond to the spectral indices of Kolmogorov, Iroshnikov and Kraichnan, and Burgers turbulence, respectively. Because of the dominance of SN shocks, both the solenoidal and compressible spectra have inertial ranges with spectral indices that are close to 2.

Figure 9 (*top*) shows the absolute value of the magnetic helicity spectrum at various times in the simulation. Figure 9 (*bottom*) shows similar spectra for the kinetic helicity. We see quite clearly that, despite their jaggedness, the magnetic helicity spectra show a secular increase with increasing time, consistent with the growth in magnetic energy. Figure 9 (*bottom*) shows no such secular increase. These results are consistent with Figure 5, which shows that the rms fluctuations in
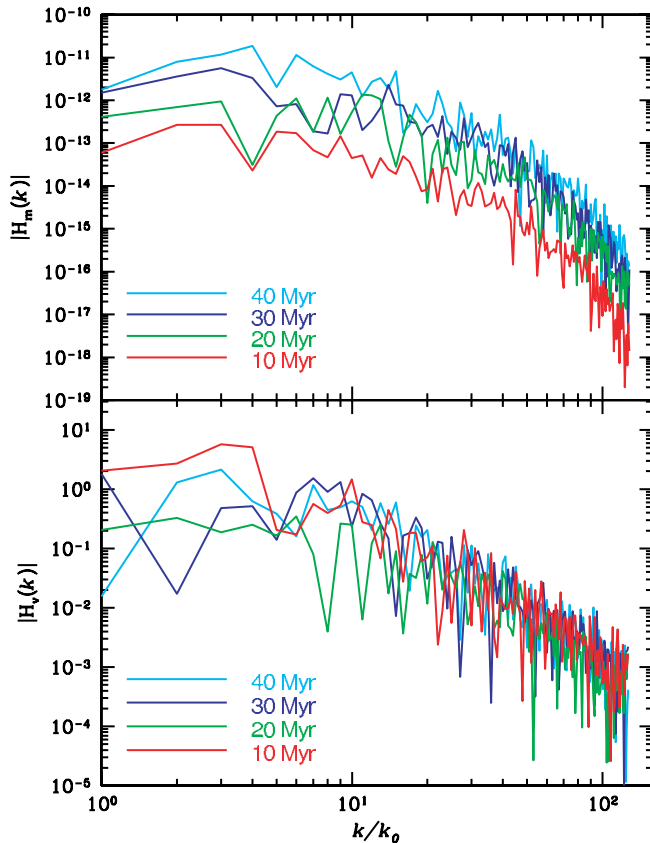
Fig. 9.—Absolute value of the magnetic (*top*) and kinetic (*bottom*) helicity spectra at various times in the simulation. Despite their jaggedness, the magnetic helicity spectra show a secular increase with increasing time, consistent with the growth of magnetic energy. The kinetic helicity shows no such secular increase.

the kinetic helicity do not show secular growth as a function of time, while the rms fluctuations in the magnetic helicity do indeed show secular growth as a function of time.

5. STRUCTURES AND STATISTICS OF THE TURBULENCE

Figure 10 shows images of the log of thermal and magnetic pressure and of the log of kinetic helicity and magnetic helicity on a slice plane that passes through a recent remnant (the one at the bottom of the panel). This particular remnant exploded in a rather low density environment. The kinetic helicity is colored so that large negative values of the helicity appear dark blue, while large positive values of the helicity appear deep red. The figures correspond to a time of 20 Myr, by which time the simulated ISM is strongly turbulent. We observe that the remnant is not spherical, and in this strongly turbulent environment, the remnant is even more aspherical than the remnants simulated in BBC01. The turbulence that gets established in the simulations reported here is much stronger than the turbulence in BBC01. As a result, we see substantially more aspherical evolution in the SN remnants simulated here than in BBC01. The images for the thermal pressure and kinetic helicity in Figure 10 when taken together clearly show that the largest fluctuations in the kinetic helicity are somewhat correlated with the remnant. It is, however, noteworthy that there are many other locations in the simulation that are disjoint from the remnant and also show quite large fluctuations in kinetic helicity. Figure 10 shows that the magnetic field does get compressed at the remnant's boundaries. However, strongly magnetized large-scale structures are visible in all parts of the domain. This shows us in a very graphical fashion that growth of magnetic field structures has taken place all over the computational domain. The magnetic helicity in Figure 10 shows substantial correlation with the magnetic energy, as expected. A similar result was also found in BBC01.

6. DISCUSSION AND CONCLUSIONS

6.1. *Discussion*

The mechanisms for field generation demonstrated here are potentially very useful in explaining the strong magnetic fields observed in our Galactic center, in starburst galaxies, and in protogalactic environments. That is especially so because the centers of disk galaxies do not have strong shear flows. In light of that fact, one is inclined to ask whether a critical SN rate that is somewhere in the range of 12–40 times the Galactic rate should be viewed as a hard limit for magnetic field amplification. There are many astrophysical effects that suggest otherwise. First, the Galactic center, as well as the centers of starbursts and protogalaxies, has considerably denser gas that might be able to contain the remnants more efficiently without undergoing thermal runaway. Second, the stratification introduces preferred channels along which hot gas may leave the system. The existence of such preferred channels might also help dynamo action because it permits small-scale tangled magnetic fields to leave the system as suggested by Blackman & Field (2000) and Kulsrud (1999). Third, fueling by bars might also dredge in new molecular gas, which might help keep the mean temperature low. Thus, an SN rate that is 12 times the Galactic SN rate should not be viewed as a hard bound. Even starburst systems such as Arp 220 that have very high rates of star formation in their centers might be able to draw on this mechanism. A similar result could hold true for protogalaxies.

KA92 point out that the fundamental problem with applying mean field dynamo theory to our Galaxy stems from the fact that our Galaxy is a system with a very high Reynolds number. They argue that the high Reynolds number causes the small-scale magnetic energy in the turbulence to quench the small-scale helical flows in the turbulent velocity field. Their argument remains valid for any weakly driven turbulence. Our SN-driven turbulence simulations show that the Galaxy might be able to bypass the limitation because SN-driven shocks are strong at small scales and so may not be subject to such α-quenching arguments.

Recent EGRET gamma-ray observations show that it is difficult to find a source for the strong magnetic fields observed in the intracluster medium (ICM) of various clusters (Dolag et al. 1999). However, Kim et al. (1991) have made observations of the magnetic field in clusters. It might be pointed out that galaxies in a cluster are strongly susceptible to tidal interactions, which is a strong source of central fueling and starburst activity. Prolific and episodic starburst activity in the ICM can also amplify the magnetic field in the ICM. The superwinds have temperatures of 10^8 K (Suchkov et al. 1994). When these superwinds plow through the ICM, which has a much lower temperature of 10^6–10^7 K, they have an effect that is similar to the interaction of SN shells with the ISM. Thus, a mechanism such as the one proposed here may also apply to the generation of magnetic fields in the ICM. It is also worth pointing out that Balsara et al. (1994) have also studied the turbulent wakes of galaxies that propagate through the ICM. They found that the turbulent wakes are indeed strong sources
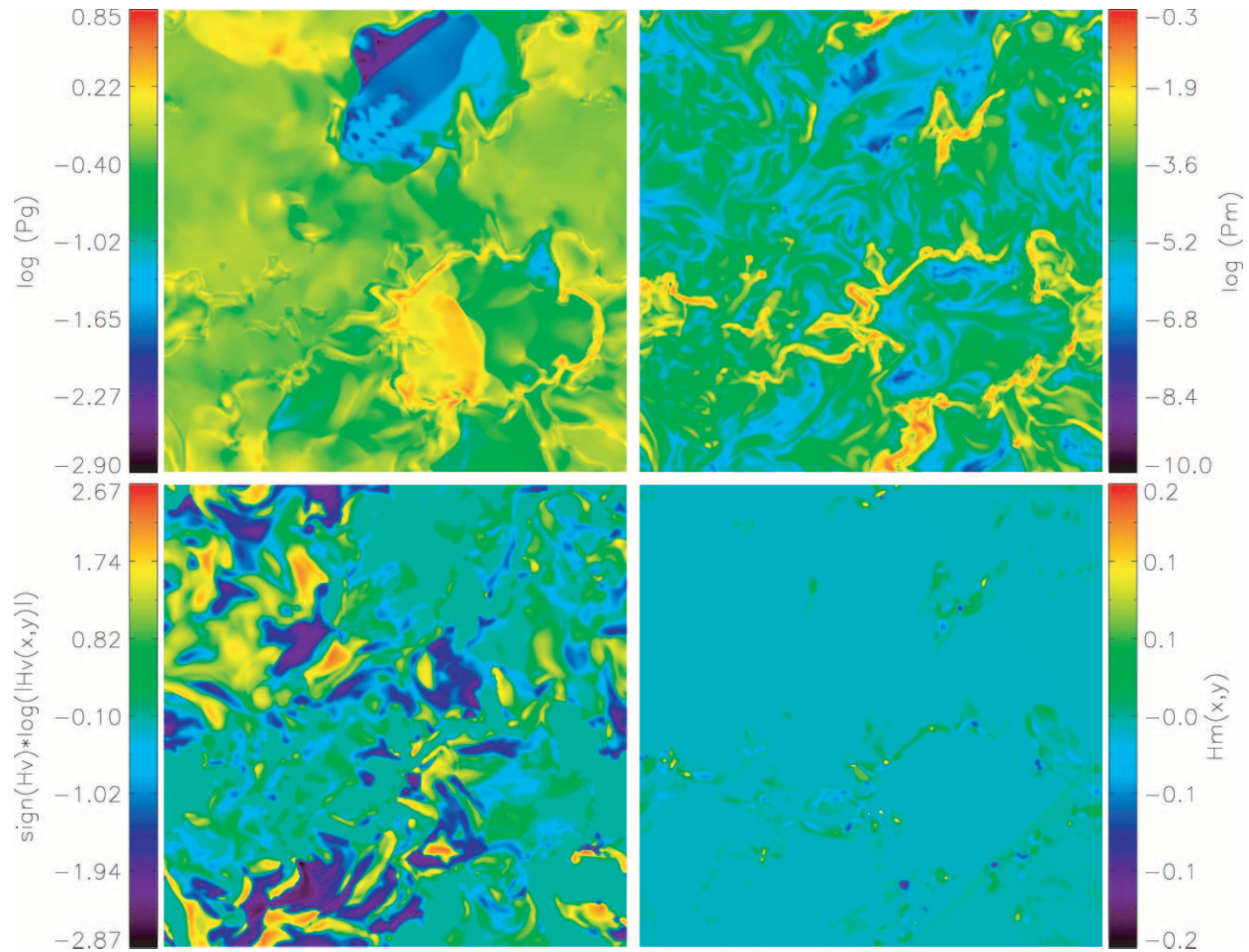
Fig. 10.—Log of the thermal (*top left*) and magnetic (*top right*) pressure, of the signed log of the kinetic helicity sign (H_v) log ($|H_v(x, y)|$) (*bottom left*), and of the magnetic helicity (*bottom right*) in a slice plane that passes through the recent remnant at the bottom of the image. Note that the magnetic helicity is not logarithmically scaled.

of vorticity and helicity. Thus, there are several mechanisms available for sustaining turbulence in the ICM.

Molecular clouds probably contain supersonic, trans-Alfvénic turbulence (see Crutcher 1999), indicating that the magnetic fields are roughly close to their equipartition values. Kornreich & Scalo (2000), Mac Low & Klessen (2004), Elmegreen & Scalo (2004), and Scalo & Elmegreen (2004) mention that strong shocks associated with high Mach number winds and jets in molecular clouds might play a role in sustaining the turbulence in molecular clouds. Molecular clouds are made clumpy by the turbulent compression and gravitational collapse of protostellar cores (Mac Low 1999; Balsara et al. 2001b). Thus, the interaction of strong shocks with the clumpy molecular cloud material could operate in a fashion that is analogous to SN shocks propagating through the clumpy ISM. It is therefore possible that shock-driven turbulence in molecular clouds plays an important role in field amplification there.

6.2. Conclusions

This work provides several new insights into the problem of magnetic field amplification in a strongly turbulent environment.

1. The SN-driven, turbulent, multiphase ISM possesses one of the major features needed for the operation of a fast dynamo: a robust and persistent helicity generation mechanism. This implies that there are many interesting astrophysical systems in which it is possible to produce such flows.

2. We confirm the report of BBC01 that strong SN shocks interacting with background interstellar turbulence produce large kinetic helicity fluctuations about a zero mean. In our model the turbulence is self-consistently generated by the SNe rather than having been generated by a uniform driver. The helicity fluctuations come about because of the amplification of turbulence in a strong shock and also because shocks propagating through a clumpy and turbulent medium naturally generate vorticity and helicity.

3. Seed magnetic fields amplify rapidly in such environments. The magnetic energy grows with growth times that are a small multiple of the eddy turnover time in the simulated system. In the linear phase of growth, different Fourier modes of the magnetic field with length scales both larger and smaller than the effective forcing scale grow at the same rate.

4. The quasi-linear phase of evolution (as defined by ZPP98), in which the initially fast linear growth of field is slowed down, sets in when the magnetic energy is about 1% of the fluid kinetic energy. This suggests that most of the growth in the protogalactic magnetic energy takes place rapidly during the linear phase of growth.

5. Spectral analysis of the flow field reveals that the solenoidal part of the total kinetic energy exceeds the compressible part of the total kinetic energy by almost an order of magnitude at most scales. It is remarkable that even though the ISM is kept turbulent by strongly compressible motions, the resulting supersonic turbulence has so much kinetic energy in solenoidal motions.

6. Our results may help explain why damped Lyα systems have strong observed magnetic fields and how protogalaxies can rapidly amplify their seed magnetic fields. Rapid magnetic field generation in molecular clouds, the Galactic center, starburst galaxies, and even in intracluster gas can be explained using the results discussed here.

REFERENCES

Balsara, D. S. 2000, Rev. Mex. AA, 9, 92
———. 2004, ApJS, 151, 149
Balsara, D. S., Benjamin, R., & Cox, D. P. 2001a, ApJ, 563, 800 (BBC01)
Balsara, D. S., & Kim, J. S. 2004, ApJ, 602, 1079
Balsara, D. S., Livio, M., & O'Dea, C. P. 1994, ApJ, 437, 83
Balsara, D. S., & Pouquet, A. 1999, Phys. Plasmas, 6, 89
Balsara, D. S., & Spicer, D. S. 1999a, J. Comput. Phys., 148, 133
———. 1999b, J. Comput. Phys., 149, 270
Balsara, D. S., Ward-Thompson, D., & Crutcher, R. M. 2001b, MNRAS, 327, 715
Beck, R., Brandenburg, A., Moss, D., Shukurov, A., & Sokoloff, D. 1996, ARA&A, 34, 155
Biermann, L. 1950, Z. Nat., 5a, 65
Blackman, E. G., & Field, G. B. 2000, ApJ, 534, 984
Boldyrev, S. 2002, ApJ, 569, 841
Childress, S., & Gilbert, A. 1995, Stretch, Twist, Fold: The Fast Dynamo (Springer: Berlin)
Churchill, C. W., & Le Brun, V. 1998, ApJ, 499, 677
Cox, D. P., & Smith, B. W. 1974, ApJ, 189, L105
Crutcher, R. M. 1999, ApJ, 520, 706
Dolag, K., Bartelmann, M., & Lesch, H. 1999, A&A, 348, 351
Elmegreen, B. G., & Scalo, J. 2004, ARA&A, 42, 211
Ferrière, K. 1993a, ApJ, 404, 162
———. 1993b, ApJ, 409, 248
———. 1995, ApJ, 441, 281
———. 1998, A&A, 335, 488
Ferrière, K., & Schmitt, D. 2000, A&A, 358, 125
Field, G. B., Goldsmith, D. W., & Habing, H. J. 1969, ApJ, 155, L149
Fosalba, P., Lazarian, A., Prunet, S., & Tauber, J. A. 2002, ApJ, 564, 762
Gaensler, B. M., Dickey, J. M., McClure-Griffiths, N. M., Green, A. J., Wieringa, M. H., & Haynes, R. F. 2001, ApJ, 549, 959
Galloway, D. J., & Proctor, M. R. E. 1992, Nature, 356, 691
Han, J. L., Ferrière, K., & Manchester, R. N. 2004, ApJ, 610, 820
Haverkorn, M., Katgert, P., & de Bruyn, A. G. 2000, A&A, 356, L13
Howard, A. M., & Kulsrud, R. M. 1997, ApJ, 483, 648
Kim, J. S., Balsara, D. S., & Mac Low, M.-M. 2001, J. Korean Astron. Soc., 34, 333
Kim, K.-T., Kronberg, P. P., & Tribble, P. C. 1991, ApJ, 379, 80
Kornreich, P., & Scalo, J. 2000, ApJ, 531, 366
Korpi, M. J., Brandenburg, A., Shukurov, A., Tuominen, I., & Nordlund, Å. 1999, ApJ, 514, L99
Kraichnan, R., & Nagarajan, S. 1967, Phys. Fluids, 10, 859
Kronberg, P. P. 1995, Nature, 374, 404
Kronberg, P. P., & Perry, J. J. 1982, ApJ, 263, 518
Kulsrud, R. M. 1999, ARA&A, 37, 37

Kulsrud, R. M., & Anderson, S. W. 1992, ApJ, 396, 606 (KA92)
Kulsrud, R. M., Cen, R., Ostriker, J. P., & Ryu, D. 1997, ApJ, 480, 481
Ledoux, C., Srianand, R., & Petitjean, P. 2002, A&A, 392, 781
Mac Low, M.-M. 1999, ApJ, 524, 169
Mac Low, M.-M., Balsara, D., Avillez, M. A., & Kim, J. S. 2004, ApJ, submitted (astro-ph/0410734)
Mac Low, M.-M., & Klessen, R. S. 2004, Rev. Mod. Phys., 76, 125
Mac Low, M.-M., & McCray, R. 1988, ApJ, 324, 776
Magnier, E. A., Chu, Y.-H., Points, S. D., Hwang, U., & Smith, R. C. 1996, ApJ, 464, 829
Maron, J., & Blackman, E. G. 2002, ApJ, 566, L41
McCray, R., & Kafatos, M. 1987, ApJ, 317, 190
McKee, C. F., & Ostriker, J. P. 1977, ApJ, 218, 148
McKee, C. F., & Zweibel, E. G. 1995, ApJ, 440, 686
McKenzie, J. F., & Westphal, K. O. 1968, Phys. Fluids, 11, 2350
Minter, A. H., & Spangler, S. R. 1996, ApJ, 458, 194
Mushotzky, R. F., & Loewenstein, M. 1997, ApJ, 481, L63
Parker, E. N. 1971, ApJ, 163, 255
Passot, T., & Pouquet, A. 1987, J. Fluid Mech., 181, 441
Perry, J. J., Watson, A. M., & Kronberg, P. P. 1993, ApJ, 406, 407
Porter, D. H., Pouquet, A., Sytine, I., & Woodward, P. R. 1999, Physica A, 263, 263
Pouquet, A., Frisch, U., & Léorat, J. 1976, J. Fluid Mech., 77, 321
Rand, R. J., & Kulkarni, S. R. 1989, ApJ, 343, 760
Rand, R. J., Kulkarni, S. R., & Hester, J. J. 1990, ApJ, 352, L1
Raymond, J. C., & Smith, B. W. 1977, ApJS, 35, 419
Ruzmaikin, A. A., Shukurov, A. M., & Sokolov, D. D. 1988, Magnetic Fields of Galaxies (Dordrecht: Kluwer)
Samtaney, R., & Zabusky, N. J. 1994, J. Fluid Mech., 269, 45
Scalo, J., & Elmegreen, B. G. 2004, ARA&A, 42, 275
Spangler, S. 1999, in Interstellar Turbulence, ed. J. Franco & A. Carraminana (Cambridge: Cambridge Univ. Press), 41
Steenbeck, M., Krause, F., & Radler, G. 1966, Z. Nat., 21a, 369
Suchkov, A., Balsara, D. S., Heckman, T., & Leitherer, C. 1994, ApJ, 430, 511
Vainshtein, S. I., & Zeldovich, Ya. B. 1972, Soviet Phys.–Uspekhi, 15, 159
Vestuto, J. G., Ostriker, E. C., & Stone, J. M. 2003, ApJ, 590, 858
Vishniac, E. T. 1983, ApJ, 274, 152
Williams, R. M., Chu, Y.-H., Dickel, J., Smith, R. C., Milne, D. K., & Winkler, P. F. 1999, ApJ, 514, 798
Wolfe, A. M., Lanzetta, K. M., & Oren, A. L. 1992, ApJ, 388, 17
Wolfire, M. G., McKee, C. F., Hollenbach, D., & Tielens, A. G. G. M. 1995, ApJ, 443, 152
———. 2003, ApJ, 587, 278
Zeinecke, E., Politano, H., & Pouquet, A. 1998, Phys. Rev. Lett., 81, 4640 (ZPP98)